



# Advanced Sensor Technology Based on Oxide Thin Film—MEMS Integration

HARRY L. TULLER

*Department of Materials Science and Engineering, Massachusetts Institute of Technology, Cambridge, MA 02139, USA*

RICHARD MLCAK

*Boston MicroSystems, Inc., Woburn, MA 01801, USA*

**Abstract.** Many of the most significant advances in achieving improved sensor performance have been tied to the integration of thin film oxides with micromachined and microelectronic technologies (MEMS). Arrays of microcantilever beams or microhotplates show great promise as chemical sensor platforms exhibiting enhanced selectivity and markedly reduced power dissipation. Microcantilever beams demonstrate exceptional sensitivity to chemical, thermal and other physical stimuli. Microhotplates, provide the opportunity to discriminate between chemical species by control of reaction rates. We review recent key developments in the micromachining of suitable structures, the means for incorporating active oxide films and the performance of individual and arrays of sensor devices.

**Keywords:** sensor, MEMS, microcantilever beam, microhotplate, electroceramics

## 1. Introduction

The ability to quickly process information for monitoring and ultimately controlling various processes has become essential in many key fields including manufacturing, environmental monitoring, health care, automotive and aerospace. So called feedback control, as illustrated in Fig. 1, depends on the availability of appropriate input and output transducers commonly designated as sensors and actuators working in concert with the “brain” of the system, the microprocessor. While microprocessors and the requisite analog to digital converters have been available for some decades, sensor and actuator technology has continued to lag, particularly with regard to achieving adequate sensitivity, reproducibility, and stability at reasonable cost. For increasing numbers of applications, additional criteria must be satisfied including (a) miniaturization and low power drain for portable and/or implanted devices, (b) arrays of devices for improved spatial or species discrimination and (c) integrated circuitry (logic, amplification,

telemetry, etc.) for enhanced functionality [1]. Advances in the micromachining of miniature three dimensional microelectromechanical structures (MEMS) including cantilever beams, bridges, membranes, channels and valves have created many opportunities for novel or improved sensors and actuators. In this paper, we discuss how the versatility of sensor and actuator devices can be significantly enhanced by the integration of active oxide thin films with MEMS technology.

Key sensor requirements are explicitly satisfied by the nature of MEMS devices. MEMS are largely fabricated by the same batch processes used for microelectronic device fabrication thereby satisfying the requirements for miniaturization and low cost. Integration of electronics and micromechanical structures on a single chip provides added functionality characteristic of smart structures. Other less obvious features include: low power dissipation during heating of low thermal mass elements, high sensitivity connected with displacement of compliant elements and enhanced chemical selectivity realized

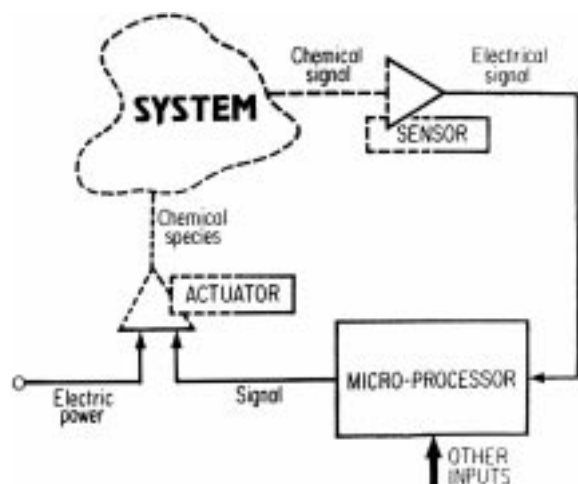


Fig. 1. Schematic of a feedback control system emphasizing need for sensors and actuators capable of translating other forms of energy (in this example, chemical) into and from electrical energy, the language of the microprocessor.

by fabricating arrays of devices with differing reactivities

While MEMS devices serve as ideal platforms for sensors, they often cannot provide the required sensitivity to physical, chemical or biological inputs of interest when fabricated only from standard materials (Si, SiO<sub>2</sub>, Si<sub>3</sub>N<sub>4</sub>, Al, etc.). Oxides, as a family of compounds, exhibit a wide range of properties (piezoelectric, pyroelectric, electro-optic, ferromagnetic and semiconductive) making them inherently useful for measuring (a) mechanical, (b) optical, (c) electrical, (d) magnetic, (e) thermal, (f) chemical and (g) biological properties. Furthermore, given the rapid progress, over the past decade, in deposition of high quality and reproducible oxide films onto silicon substrates, e.g., high  $T_C$  superconductors, high dielectric constant dielectrics and ferroelectrics [2], integration of oxide thin films with MEMS provides unique opportunities for developing unique sensor and actuator systems. The intersection of microelectronics, micromechanics and electroceramics, as illustrated in Fig. 2, creates unique new options for microsystems designs which include sense, signal processing, telemetry and actuation functions. In the following we focus on two structures, microcantilever beams and microhotplates, which show particular promise as sensor platforms. Furthermore, rather than providing a broad coverage

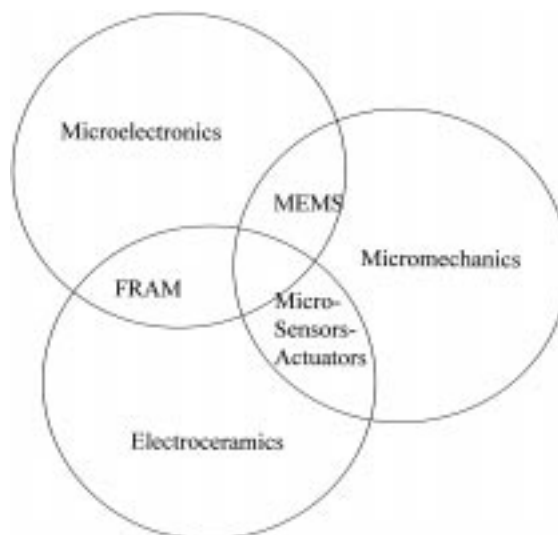


Fig. 2. The intersection of the three rings representing microelectronics, micromechanics and electroceramics creates a new field of sensor and actuator devices with exceptional functionality and versatility. FRAM, the acronym for nonvolatile ferroelectric random access memories, is one example of electroceramics-microelectronics integration providing a new technology dependent on the unique characteristics of oxide films.

of many types of sensors, we concentrate our attention on chemical sensor technology based on oxide thin film-MEMS integration.

## 2. Chemical Sensors

The most common means for detection of chemical or gaseous species are based on (1) electrical resistivity, (2) mechanical deflection or (3) resonance principles. We describe below how these principles are being applied in the development of MEMS based devices.

### 2.1. Resistive

The electrical conductivity of oxide films may be modified by the adsorption of molecules on their surfaces and, at higher temperatures, the diffusion of oxygen into or out of the film interior. It is well known that lattice defects such as vacancies and interstitials on either metal or oxygen sites can serve as donors or acceptors (i.e., oxygen vacancies and metal interstitials serve as donors while oxygen interstitials or

metal vacancies serve as acceptors). Thus, for example, subjecting an oxide film, such as  $\text{SnO}_2$ , to decreasing oxygen partial pressure ( $P_{\text{O}_2}$ ) at kinetically favorable temperatures will lead to increasing levels of oxygen deficiency and consequently increasing levels of  $n$ -type conductivity. Applying defect chemical concepts [3], it is straight forward to show that  $\log$  conductivity has the following linear dependence on  $\log P_{\text{O}_2}$ ,

$$\log \sigma = K(T) + x \log P_{\text{O}_2} \quad (1)$$

This type of dependence is well illustrated in Fig. 3 showing the results of our studies on the pyrochlore oxide  $\text{Gd}_2\text{Ti}_2\text{O}_7$ . Several features are noteworthy. First, the value of  $x \approx -1/6$  strongly supports a model in which the electron carrier generation mechanism is by double ionization of oxygen vacancy donors [4]. These results depend on there being adequate time for oxygen to diffuse from the center of the specimen to an outside surface and thereby equilibrate with the surrounding atmosphere. Given that oxygen diffusivity decreases exponentially with decreasing temperature, the time to reach equilibrium correspondingly increases exponentially with decreasing temperature. Thus, resistive gas sensors

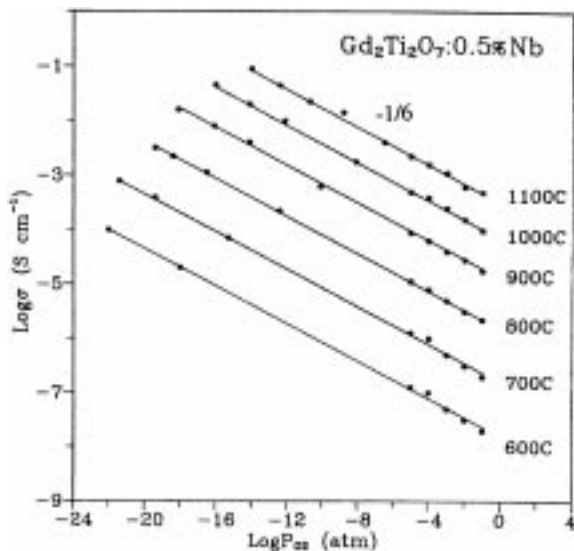


Fig. 3. The  $P_{\text{O}_2}$  dependence of the electrical conductivity of the pyrochlore  $\text{Gd}_2\text{Ti}_2\text{O}_7$  doped with 0.5% Nb shows a single well defined  $-1/6$  slope over a wide range of temperatures (600–1100°C) demonstrating promise as a resistive gas sensor material [4].

which depend on changes in their bulk resistance must be operated at sufficiently elevated temperatures and/or be very thin or highly porous [3].

Alternatively, lower temperature operation may be achieved by relying solely on changes induced in the surface conductivity of films due to the adsorption and desorption of gaseous species. For example, oxygen being an electronegative species, acts as an electron trap when adsorbed onto an oxide surface. This serves to deplete electrons from  $n$ -type and induce accumulation of holes in  $p$ -type semiconducting oxides, respectively. This modulation of the space charge region, in turn, modulates the oxide's surface conductivity. This same principle is sometimes used to modulate the grain boundary resistance of a porous specimen, or the contact resistance of a metal/semiconducting oxide Schottky barrier. The gas selectivity of these devices to gases like  $\text{CO}$ ,  $\text{H}_2$  or  $\text{CH}_4$  can be improved by coating the oxide surface with catalysts or by changing the temperature to catalyze certain reactions at the expense of others. Devices based on  $\text{SnO}_2$  coated with a variety of catalysts are now commercially available. While exhibiting adequate sensitivity, these self heated devices, nevertheless, suffer from relatively high power dissipation ( $\approx 1\text{W}$ ) and inadequate selectivity.

MEMS technology promises to overcome such limitations. Thin membranes (3–10  $\mu\text{m}$  thick) are now routinely prepared on silicon wafers by a variety of micromachining techniques. While such membranes are most commonly used in the fabrication of pressure sensors, they can serve as low thermal mass supports for gas sensitive oxide films as illustrated in Fig. 4 [5]. Here, a  $\text{SnO}_2$  film, interdigitated electrodes, and resistive heater are fabricated on the membrane. The  $\text{SnO}_2$  is applied by spinning on a metal-organic precursor followed by a thermal anneal. Because of its low thermal mass, the temperature of the sensor can be readily modulated as shown in Fig. 5. This is particularly significant given that  $\text{SnO}_2$  and related oxide sensors cannot readily discriminate between similar gaseous species, e.g., hydrocarbons at a given temperature. However, the sensor's response to a given gas is quite temperature dependent. Indeed, Wu and Ko [5] clearly demonstrated that the temperature response "finger print" of each of a number of closely related anesthetic agents was quite distinct (Fig. 5) even if the magnitude of the sensor output for each of the

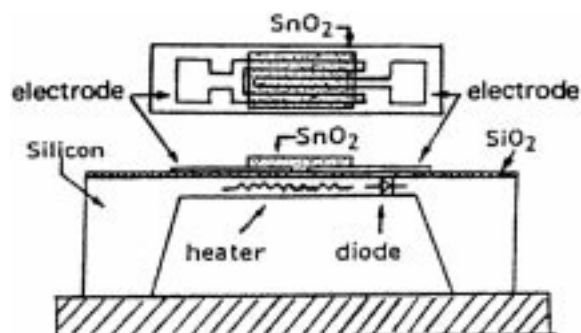


Fig. 4. Gas microsensor based on a thin semiconducting  $\text{SnO}_2$  film deposited on a thin, heated Si micromachined membrane [5].

gases, at any given temperature, was not very different.

More recently, this concept has been further exploited by forming so called "microhotplates." One design being used by the group at NIST is illustrated in Fig. 6. A key distinction is in the use of thin tethers or support beams which thermally isolate the hotplate and sensor element from the remainder of

the wafer. This leads to much higher thermal efficiency ( $8^\circ\text{C}/\text{mW}$ ), faster thermal rise and fall times, and higher maximum operating temperatures ( $500\text{--}800^\circ\text{C}$ ). Semancik and Cavicchi [6] report the use of micromachined, low mass ( $\sim 0.2\mu\text{g}$ ) suspended microhotplates to rapidly cycle the temperature of sensor films deposited on these structures at millisecond thermal rise and fall times. Such cycling enables "kinetic" differentiation of chemical species by their unique temperature-response signatures. Figure 7 shows the temperature programmed response of tin oxide microsensors to a number of different solvents, demonstrating that distinct thermal signatures are achieved for each solvent. Nakata et al. [7] also report enhanced differentiation among gases by examination of conductance variations of sensors operating under sinusoidal thermal cycling. Ratton et al. [8] discuss the use of network and clustering methods for developing recognition algorithms which can be applied to enhance analyte recognition. Thermal isolation of the low mass microhotplates from the remainder of the chip enables cyclic heating of the

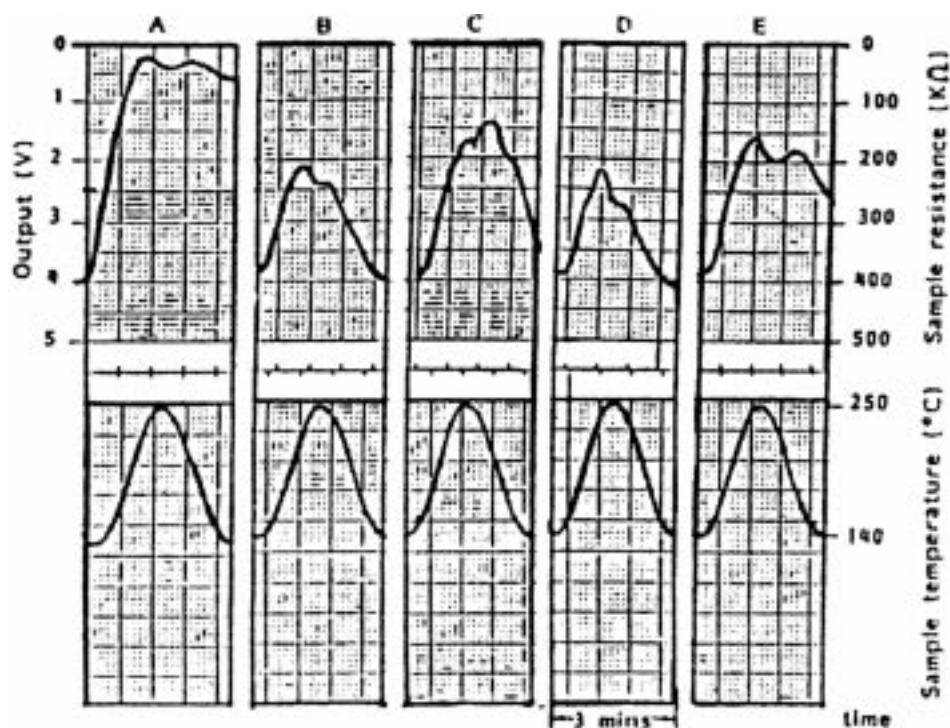


Fig. 5. Waveforms representing the response of the sensor illustrated in the above figure to anesthetic agents with sinusoidal temperature-time curves. A, alcohol; B, halothane; C, ethyl-ether; D, forane; E, pentane, all at 200 ppm levels [5].

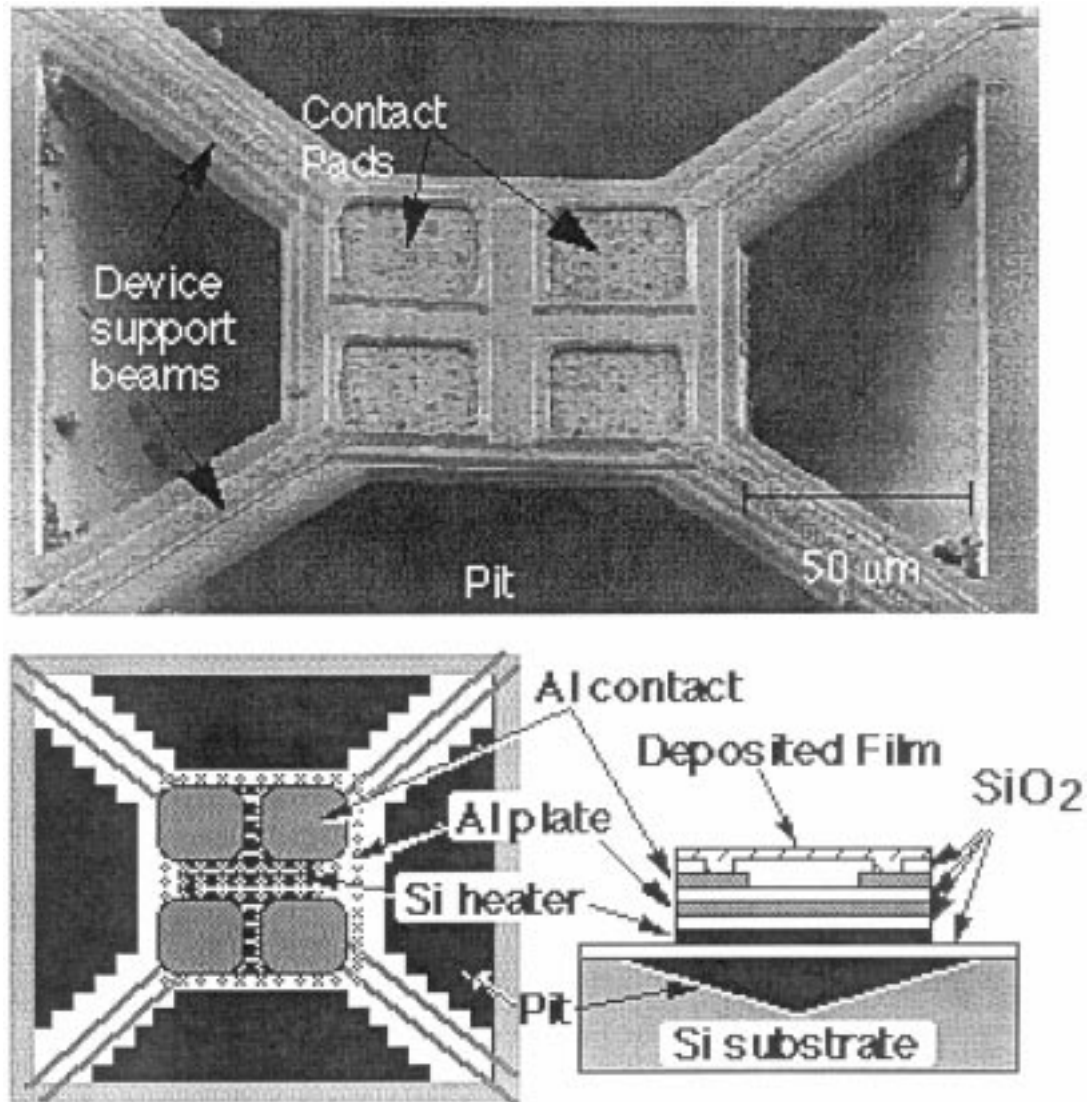


Fig. 6. The top image is an SEM micrograph of a suspended microhotplate structure with an SnO<sub>2</sub> film coating. The lower half shows schematics of the various layers comprising the structure [9].

sensors at only a fraction of the power required by bulk devices ( $500 \mu\text{W}$ – $40 \text{ mW}$  vs.  $1 \text{ W}$ ) [9,10], of critical importance for portable operation.

The use of microhotplate arrays having differing sensor films provides further capability for identifying and distinguishing analytes, as no two film compositions respond identically to the same gases. Self lithographic metalorganic chemical vapor deposition (MOCVD) has been used to selectively deposit sensor films onto individual microhotplates, by taking advantage of the thermally activated nature of

MOCVD and the ability to individually heat selected microhotplate heaters to specified temperatures [11]. Furthermore, the sensitivity and selectivity of resistive sensors can be significantly modified by treating surfaces with additives such as Pt, Pd and Ru [12,13]. Thus, arrays of even partially selective elements can be combined to provide overall enhanced selectivity [14]. Sensor arrays with as many as 48 elements are under development [6].

Applications exist, particularly for use in auto exhaust and catalytic converters [15], for which

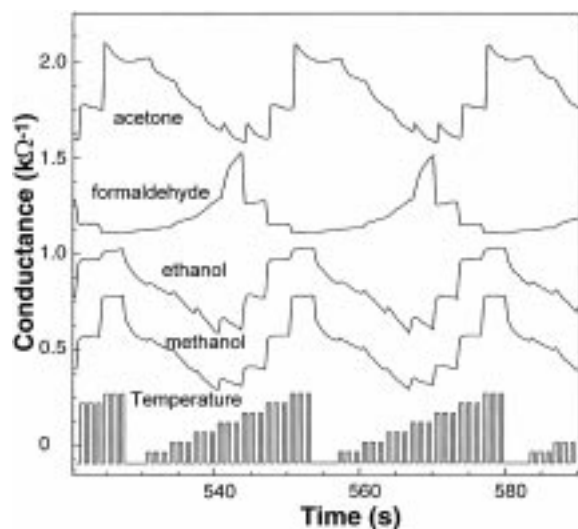


Fig. 7. Temperature programmed response of tin oxide microhotplate sensors to a series of organic vapors. Note the distinct signatures. From reference [6].

sensor operation at elevated temperatures is beneficial or required. Operation at elevated temperatures (a) minimizes effects of microstructure on response as recently demonstrated for  $\text{BaSnO}_3$ , (b) lowers response times to the millisecond regime, (c) eliminates cross sensitivity to humidity, (d) and improves cold-start engine behavior.  $\text{SrTiO}_3$  exhibits high temperature stability and rapid oxygen diffusion making it particularly attractive as a lambda probe for monitoring the transient response of individual cylinders [15].  $\text{Ga}_2\text{O}_3$  equilibrates with the gas phase above  $900^\circ\text{C}$  and changes its conductivity accordingly, while remaining resistant to long term  $\text{SO}_2$  exposure [16,17]. While microhotplate sensors fabricated from silicon cannot operate at these temperatures, recent progress, by the authors, in the micromachining of SiC [18] promises to extend this technology to this important temperature regime.

## 2.2. Mechanical Deflection and Resonance

Scanning probe microscopy has highlighted the use of an alternative MEMS technology based on microcantilever beams (MCB). With recent advances in microfabrication technologies, cantilever beams can be reproducibly fabricated with precise dimensional control, sub-micron dimensions, and readily adjustable mechanical parameters (compliance, reso-

nance frequency) through appropriate choice of cantilever dimensions [18]. MCBs with spring constants of 0.01–100 N/m coupled with vertical displacement resolution of picometers enables detection of forces down to the pico-nano newton range. Thundat et al. [19] have demonstrated physical, chemical, and biological sensors with exceptionally high resolution based upon the microcantilever platform, by detecting changes in cantilever static deflection or resonant response. Precise cantilever beam deflection can be measured, for example, by: (1) reflection of a focused laser beam from the cantilever surface onto a position sensitive photodiode, (2) the stress-induced change in resistance of piezoresistive elements on the cantilever, (3) a change in capacitance between the cantilever beam and a reference element.

Chemical detection at ppt-ppb sensitivities has been demonstrated using microcantilever beams coated with chemically specific layers. Chemical species adsorbed on these layers result either in surface stress induced static deflections of the beam, or a change in beam resonant frequency caused by mass loading and/or change in spring constant [19]. Alternatively, bi-material beams having a thermal expansion mismatch between the layers can be utilized to detect temperature changes induced by gas reactions on the beam's surfaces [20], as illustrated in Fig. 8. Such calorimeters are capable of detecting temperature changes of 2 mK or 40 pW of power. In a similar mode, Berger et al. [21] used

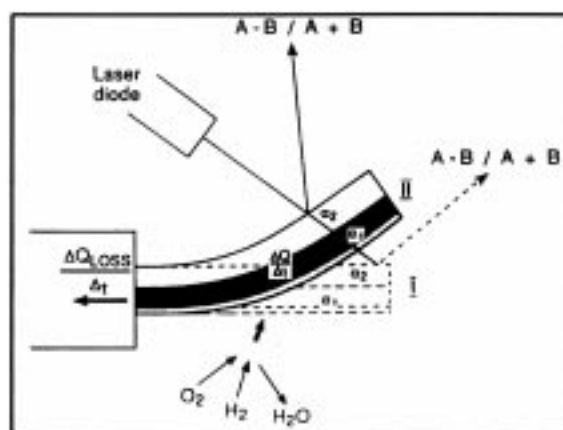


Fig. 8. A bi-material beam calorimeter showing deflection due to heat being given off by the reaction of  $\text{H}_2$  and  $\text{O}_2$  to form water [20].

bimetallic cantilever thermal sensors as micromechanical calorimeters for thermal analysis of phase transitions in picoliter samples.

For static deflection, the tip displacement  $\xi$  due to a differential stress  $\delta s$  is given by [22]:

$$\xi = \left[ \frac{3(1-\nu)L^2}{t^2E} \right] \delta s \quad (2)$$

with  $\nu$  Poisson's ratio,  $E$  Young's modulus,  $L$  the beam length and  $t$  its thickness. For small changes in mass, the resonant frequency shift of microcantilevers from  $\nu_1$  to  $\nu_2$  may be approximated by:

$$\nu_2 = \nu_1 \left[ 1 - \frac{1}{2} \frac{\delta m}{m} \right] \quad (3)$$

where  $\delta m$  is the mass change in the effective mass,  $m$ , of the beam.

Relative humidity (RH) was detected at picogram resolution with gelatin coated cantilevers using both static deflection (0.002 RH/mV as determined by error voltage) and resonant frequency (0.14 RH/Hz) [23]. In a related experiment, mercury vapor at a concentration of  $\approx 30 \mu\text{g}/\text{m}^3$  ( $\approx 20$  ppb) was measured at a sensitivity of 0.7 pg/Hz by adsorption onto gold coated cantilevers [24]. Similar results should be achievable by using selectively adsorbing oxide layers.

As for microhotplate chemical sensors, MCB sensors may be fabricated in arrays with coatings of differing selectivity or functionality. When used in conjunction with neural network analysis, highly sensitive detection and differentiation of a wide range of chemical species can be expected. Lang et al. [25] demonstrated the utility of using MCB arrays to extract small cantilever signals from noisy environments (e.g., flowing fluids, external vibrations). Signals were determined from the difference in response of Pt coated and uncoated reference MCBs. Noise averaging using 4 such cantilever pairs reduced the peak-to-peak noise amplitude by a factor of  $\approx 2$ .

As evident from Eqs. (2) and (3), critical requirements for favorable cantilever beam sensor performance include: (1) precise control of cantilever dimensions for reproducible sensor response, (2) highly reproducible mechanical properties, including low internal stress, and (3) the capability of achieving submicron dimensions and low mass as required for high sensitivity. Further improvements in sensor performance are expected to result from the ability to fabricate cantilevers with (1) optimized (more

complex) geometries, (2) integrated microheaters, thermocouples, and other complementary sensors, and (3) from materials such as silicon carbide which can operate in extreme (high temperature or corrosive) environments not suitable for silicon. In the following, we discuss some of the limitations of present micromachining technologies with respect to the fabrication of MCBs and microhotplates and the advances made by the authors utilizing a novel photoelectrochemical micromachining process utilizing *p-n* junction etch stops.

### 3. Microcantilever Beam Fabrication

Traditional bulk micromachining relies on the fact that certain chemicals, such as KOH, preferentially etch Si along specific crystallographic orientations, and that certain dopants can lower the etch rate and thus serve as etch-stops. The common etch stops include (1) the *p+* etch stop, based upon the decreased etch rate of heavily boron doped silicon in caustic solutions, and (2) the anodic passivation etch stop, based upon the  $10^2$  to  $10^3$  selectivity in etch rate between silicon and its anodic oxide. While commercially successful, these etch stops have several limitations, including: (1) low etch-stop selectivity, limiting reproducibility and tolerance control in cantilever dimensions, (2) highly stressed and electrically degenerate *p+* layers leading to curling of released structures and precluding ready incorporation of electronic functionality, (3) limited applicability to silicon, not allowing fabrication of similar structures from other semiconductors and (4) crystallographic limitations due to the unique etch anisotropy characteristic of these chemical etchants.

Many of these limitations are eliminated with the versatile photoelectrochemical (PEC) micromachining technologies developed by the authors [18,26–29]. These provide a variety of capabilities meeting key requirements including (1) precise dimensional control down to  $0.1 \mu\text{m}$  (etch selectivities in excess of  $10^7$ ), (2) negligible internal stress, (3) complex and high aspect ratio geometries unconstrained by specific crystallographic orientations, (4) rapid etch rates (up to  $100 \mu\text{m}/\text{min}$  under certain circumstances) and (5) materials versatility, e.g., Si, SiC, Ge, GaAs, GaN, etc. Details of the experimental procedures followed are published elsewhere [18]. In the following, we present examples of micromachined

cantilevers illustrating the ability to satisfy the requirements of high resolution microcantilever sensors.

Precise dimensional control is critical for reproducible cantilever sensor response. For example, cantilever beam deflections are inversely proportional to thickness squared as seen in Eq. (2). The ability to precisely control cantilever beam dimensions using photoelectrochemical (PEC) p-n junction etch-stops is demonstrated in Fig. 9, in which the beam tolerances are limited by the dimensional tolerances of standard

microelectronics processes (lithography, diffusion, epitaxial growth, etc.). Submicron dimensions are required for fabricating highly compliant and/or low mass cantilevers for enhanced sensitivity. PEC p-n junction etch-stops allow fabrication of single crystal silicon microcantilevers with thicknesses of less than  $0.3 \mu\text{m}$ .

Internal stresses strongly affect cantilever deflection and resonant frequency, and have deleterious effects on the reproducibility, sensitivity, and long term stability of cantilever beam sensors. Zero initial

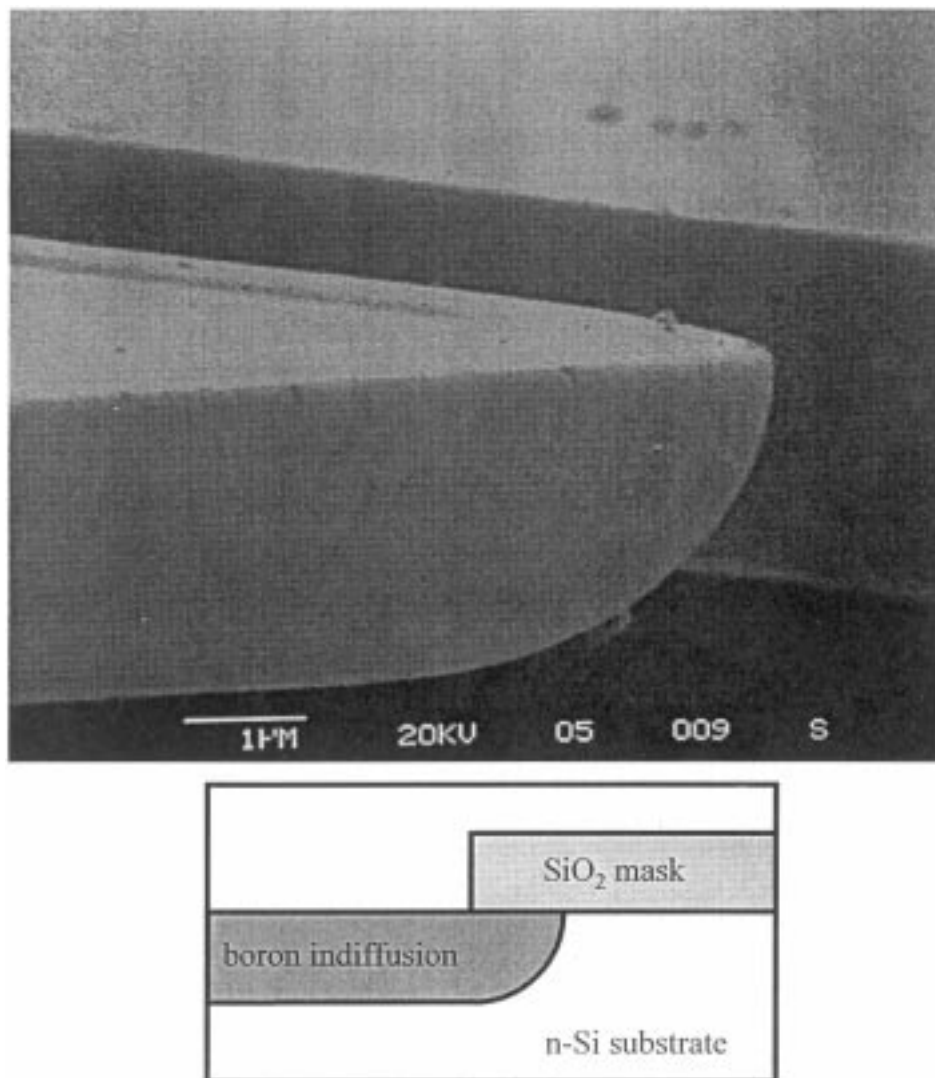
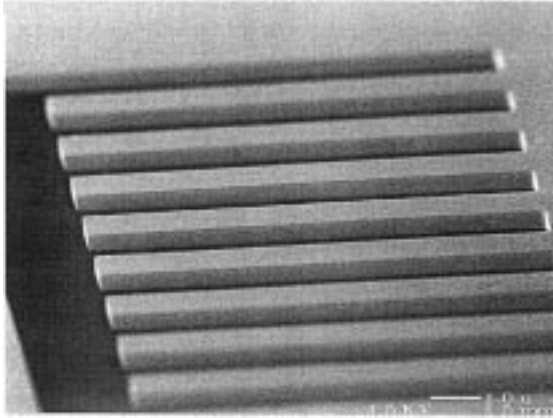


Fig. 9. SEM micrograph of PEC micromachined beam edge for which dimensions were defined by in-diffusion of boron into an n-Si wafer through a patterned oxide mask [18].





*Fig. 10.* SEM micrograph of array of stress-free MCBs fabricated in (100) silicon. Beams are  $100 \times 10 \times 5 \mu\text{m}$  [18].

deflection of beams simplifies sensor calibration and the evaluation of mechanical properties of films deposited onto them. This uniformity is particularly

significant in the operation of devices based on arrays of beams such as IR cameras. In Fig. 10 we show an array of virtually stress-free, flat microcantilevers as a consequence of the moderate and uniform doping levels used in our process.

Thin films are often deposited (e.g., by chemical vapor deposition) onto cantilevers, either as active sensor elements or as materials to be characterized. The microstructure and materials properties of these films (mechanical, electrical, chemical, optical, etc.) often depend on the crystallographic orientation of the substrate. PEC etching is a nearly crystallographically isotropic process, and enables fabrication of cantilevers on substrates of all orientation. Figure 11 shows a comparison of identical high aspect ratio cantilevers fabricated in (100) and (111) silicon wafers.

Further opportunities exist for enhancing sensor performance by tailoring the cantilever surface morphology. For example, cantilevers having high surface areas for enhanced adsorption of chemical or

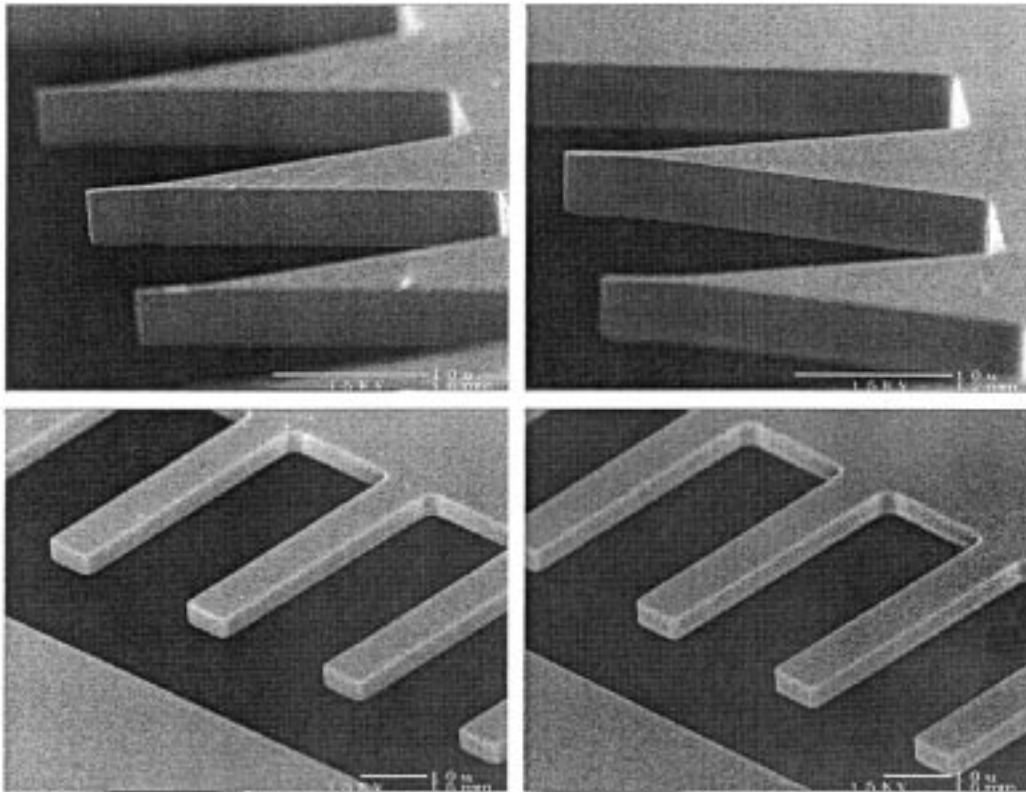


*Fig. 11.* SEM micrographs of  $4.2 \mu\text{m}$  thick MCBs fabricated in (100) silicon (left) and (111) silicon (right), showing ability to micromachine high aspect ratio beams without constraint to specific crystal plane or orientation. Beams aligned in the [100] direction (top) and [110] direction (bottom) [18].

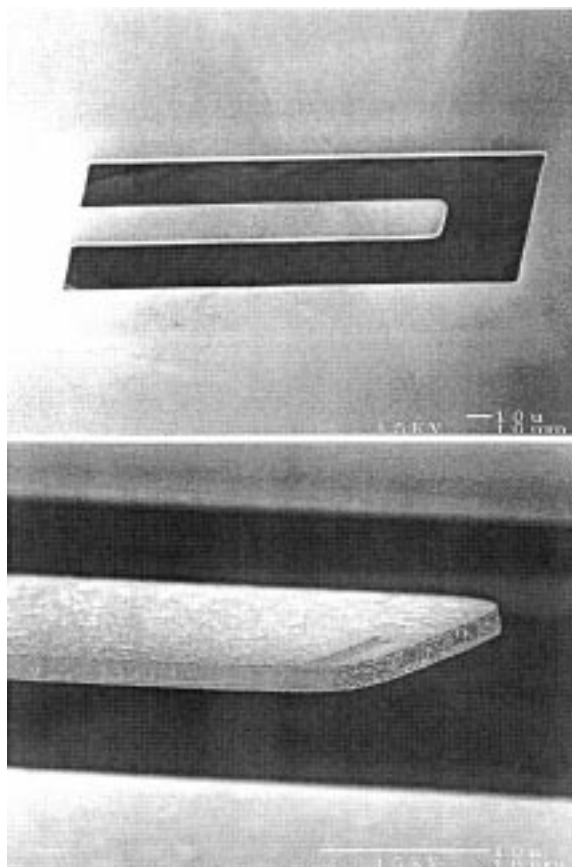


Fig. 12. SEM micrograph of a single crystal 6H-SiC MCB fabricated for the first time by the authors utilizing Boston MicroSystems' PEC micromachining technology.

biochemical species may be fabricated by anodically forming thin porous silicon layers directly on the cantilever surface.

In contrast to traditional bulk silicon micromachining processes which apply only to silicon, photoelectrochemical micromachining may be applied to many types of semiconductors. Fabrication of cantilever beams or other MEMS devices from more robust materials such as SiC or GaN holds promise for sensor applications suitable for use in extreme (high temperature or corrosive) environments. Recently, the authors successfully fabricated a single crystal 6H-SiC MCB for the first time as illustrated in Fig. 12 and are applying this technology in the development of robust sensor devices.

#### 4. Summary

Significant recent advances in sensor performance have been tied to integration of thin film oxides with micromachined and/or microelectronic technologies. Microhotplate and microcantilever beam arrays show great promise as chemical sensor platforms exhibiting enhanced selectivity and markedly reduced power dissipation. Microcantilever beam based devices have demonstrated, in some cases, orders of magnitude improvements in sensitivity. Optimum performance requires high dimensional control, reproducible properties, complex geometries and/or robust materials. Photoelectrochemical micromachining provides means for fabricating high quality microcantilever beams, microhotplates and other MEMS structures. Examples of microcantilever beams were presented which exhibited precise dimensional control, virtually no residual stress, submicron dimensions, and wafers of several crystallographic orientations. Furthermore, in contrast to traditional silicon bulk micromachining processes and etch-stops, photoelectrochemical micromachining is applicable to large gap, refractory semiconductors such as GaN, SiC and GaAs. The intersection of microelectronics, micromechanics and electroceramics, creates unique new options for microsystems designs which include the ability to integrate sense, signal processing, telemetry and actuation functions and thereby enable the development of highly functional, miniaturized feedback control systems.

#### 5. Acknowledgments

H.L. Tuller appreciates the support provided by the National Science Foundation under Award No. DMR97-01699 for sensor research. The work on MEMS-based sensors at Boston MicroSystems, Inc. was supported, in part, by the Department of Energy under grant DE-FG02-98ER82541. The authors are grateful to S. Semancik and R. Cavicchi of NIST and T. Thundat and B. Warmack of Argonne National Labs for helpful discussions.

#### References

1. H.L. Tuller and R. Mlcak, *Current Opinion in Solid State & Materials Science*, **3**, 501 (1998).

2. See other articles in this proceedings.
3. D.C. Hill and H.L. Tuller, *Ceramic Materials for Electronics*, 2nd edition, ed. R.C. Buchanan (Marcel Dekker, NY, 1991), p. 249.
4. I. Kosacki and H.L. Tuller, *Sensors and Actuators B*, **24–25**, 370 (1995).
5. Q. Wu and W.H. Ko, *Sensors and Actuators*, **B1**, 183 (1990).
6. S. Semancik and R. Cavicchi, *Accounts of Chemical Research*, **31**, 279 (1998).
7. S. Nakata, E. Ozaki, and N. Ojima, *Anal. Chem Acta*, **361**, 93 (1998).
8. L. Rattton, T. Kunt, T. McAvoy, T. Fuja, R. Cavicchi, and S. Semancik, *Sensors and Actuators B*, **41**, 105 (1997).
9. R.E. Cavicchi, J.S. Suehle, P. Chaparala, K.G. Kreider, M. Gaitan, and S. Semancik, *IEEE Solid State Sensor and Actuator Workshop* (Hilton Head, SC, 1994) p. 53.
10. A. Pike and J.W. Gardner, *Sensors and Actuators B*, **45**, 19 (1997).
11. F. DiMeo, R.E. Cavicchi, S. Semancik, J.S. Suehle, N.H. Tea, J. Small, J.T. Armstrong, and J.T. Kelliher, *J. Vac. Sci. Technol. A*, **16**, 131 (1998).
12. V.A. Chandhary, I.S. Mulla, S.R. Sainbar, A.A. Belhebar, and K. Vijayamohanan, *Sensors and Actuators A*, **65**, 197 (1998).
13. D.S. Vlachose, C.A. Papadopoulos, and J.N. Avaritsiotis, *Sensors and Actuators B*, **44**, 458 (1997).
14. A. Götze, I. Gràcia, C. Cané, E. Lora-Tamayo, M.C. Horrillo, J. Getino, C. Garcia, and J. Gutiérrez, *Ibid*, 483–487.
15. H. Meixner, J. Gerblinger, U. Lampe, and M. Fleischer, *Sensors and Actuators B*, **23**, 119 (1995).
16. M. Fleischer, M. Seth, C.D. Kohl, and H. Meixner, *Sensors and Actuators B*, **35–36**, 297 (1996).
17. M. Fleischer, M. Seth, C.D. Kohl, and H. Meixner, *Sensors and Actuators B*, **35–36**, 290 (1996).
18. R. Mlcak and H.L. Tuller, *Microstructures and Microfabricated Systems IV*, eds. P.J. Hesketh, H. Hughes and W.E. Bailey, (The Electrochemical Soc., Pennington, NJ, 1998) p. 227.
19. T. Thundat, P.I. Oden, and R.J. Warmack, *Microscale Thermophysical Engineering*, **1**, 185 (1997).
20. J.K. Gimzewski, Ch. Gerber, E. Meyer, and R.R. Schlitter, Using a Micromechanical Sensor, *Chem. Phys. Lett.*, **217**, 589 (1994).
21. R. Berger, C.H. Gerber, J.K. Gimzewski, E. Meyer, and H.J. Guntherodt, *Appl. Phys. Lett.*, **69**, 40 (1996).
22. E.A. Wachter and T. Thundat, *Rev. Sci. Instrum.*, **66**, 3662 (1995).
23. T. Thundat, G.Y. Chen, R.J. Warmack, and E.A. Wachter, *Anal. Chem.*, **67**, 519 (1995).
24. T. Thundat, E.A. Wachter, S.L. Sharp, and R.J. Warmack, *Appl. Phys. Lett.*, **66**, 1695 (1995).
25. H.P. Lang, R. Berger, C. Andreoli, J. Brugger, M. Despont, P. Vettiger, Ch. Gerber, J.K. Gimzewski, J.P. Ramseyer, E. Meyer, and H.-J. Guntherodt, *Appl. Phys. Lett.*, **72**, 383 (1998).
26. R. Mlcak, H.L. Tuller, P. Greiff, H. Sohn, and L. Niles, *Sensors and Actuators A*, **40**, 49 (1994).
27. H.L. Tuller and R. Mlcak, *Sensors and Actuators B*, **35–36**, 255 (1996).
28. R. Mlcak and H.L. Tuller, U.S. Patent 5,338,416, Aug. 16, (1994).
29. R. Mlcak and H.L. Tuller, U.S. Patent 5,464,509, Nov. 7, (1995).